

Exchanging-based Multimodal Fusion with Transformer

Renyu Zhu^{1*} Chengcheng Han^{2*} Yong Qian³ Qiushi Sun⁴

Xiang Li^{2†} Ming Gao² Xuezhi Cao³ Yunsen Xian³

¹NetEase Fuxi AI Lab, Hangzhou, Zhejiang, China

²School of Data Science and Engineering, East China Normal University, Shanghai, China

³Meituan Inc., Beijing, China ⁴National University of Singapore

zhurenyu@corp.netease.com 52215903007@stu.ecnu.edu.cn

sarahyongq@gmail.com qiushisun@u.nus.edu

{xiangli, mgao}@dase.ecnu.edu.cn {caoxuezhi, yunsenxian}@meituan.com

Abstract

We study the problem of multimodal fusion in this paper. Recent exchanging-based methods have been proposed for vision-vision fusion, which aim to exchange embeddings learned from one modality to the other. However, most of them project inputs of multimodalities into different low-dimensional spaces and cannot be applied to the sequential input data. To solve these issues, in this paper, we propose a novel exchanging-based multimodal fusion model MuSE for text-vision fusion based on Transformer. We first use two encoders to separately map multimodal inputs into different low-dimensional spaces. Then we employ two decoders to regularize the embeddings and pull them into the same space. The two decoders capture the correlations between texts and images with the image captioning task and the text-to-image generation task, respectively. Further, based on the regularized embeddings, we present CrossTransformer, which uses two Transformer encoders with shared parameters as the backbone model to exchange knowledge between multimodalities. Specifically, CrossTransformer first learns the global contextual information of the inputs in the shallow layers. After that, it performs inter-modal exchange by selecting a proportion of tokens in one modality and replacing their embeddings with the average of embeddings in the other modality. We conduct extensive experiments to evaluate the performance of MuSE on the Multimodal Named Entity Recognition task and the Multimodal Sentiment Analysis task. Our results show the superiority of MuSE against other competitors. Our code and data are provided at <https://github.com/RecklessRonan/MuSE>.

and feelings, and further fusing them. Therefore, *multimodal fusion* has become a key research problem (Baltrušaitis et al., 2018) in the area of artificial intelligence. With the recent success of deep learning, a series of deep multimodal fusion methods (Bayoudh et al., 2021; Guo et al., 2019) have been proposed and applied on various multimodal tasks, such as Multimodal Named Entity Recognition (MNER) (Sun et al., 2021; Wang et al., 2020) and Multimodal Sentiment Analysis (MSA) (Colombo et al., 2021; Wu et al., 2021). Early methods mainly can be divided into two categories: aggregation-based and alignment-based. Aggregation-based methods first represent each modality by a sub-network and then aggregate different representations with various operators, such as concatenation (Zeng et al., 2019), averaging (Hazirbas et al., 2016), and self-attention (Valada et al., 2020). Further, alignment-based methods (Colombo et al., 2021; Song et al., 2020) adopt a regularization loss to align the embeddings of different sub-networks without explicit combination.

Recently, a novel exchanging-based method CEN (Wang et al., 2020) was proposed to handle the trade-off between intra-modal processing and inter-modal fusion. By utilizing the scaling factor of Batch Normalization (BN) (Ioffe and Szegedy, 2015) as the importance measurement of each channel, CEN replaces those channels with close-to-zero factor values in one modality with the average of channels in the other modality. However, the method is specially designed for vision-vision fusion and the channel exchange cannot be directly applied in other multimodal scenarios, such as text-vision fusion. There are two main challenges. On the one hand, CEN implicitly assumes that the two modalities are represented in the same low-dimensional embedding space, while the modalities of texts and images are distant from each other and generally correspond to different spaces. On the other hand, the exchanging mode based on

1 Introduction

Humans perceive the world by simultaneously processing various modalities, such as visions, sounds

*Equal contribution

†Corresponding author

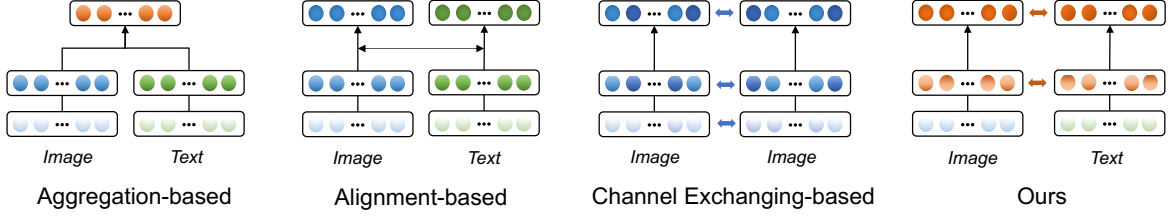


Figure 1: A sketched comparison between existing fusion methods and ours.

CNN channels of images is inapplicable for texts, since texts are sequences of words. Therefore, a research question arises: *Can we develop an effective exchanging-based neural network model that fuses modalities of text and vision?*

In this paper, we present a novel **Multimodal fuSion** method based on **Exchanging**, namely, MuSE, which bridges the gap of exchanging-based methods in the field of text-vision multimodal fusion. We summarize the comparison between existing multimodal fusion methods and ours in Figure 1. To handle the problem of different low-dimensional spaces corresponding to various data modalities, we first perform separate low-dimensional projections for texts and images, and then propose two tasks to pull their embeddings into the same space. Specifically, inspired by the fact that texts can be captions of images and images can also be generated from texts, we specially design an *image captioning* task and a *text-to-image generation* task to capture the correlations between texts and images. We implement the process with an architecture of two encoder-decoders, where encoders are used for text (image) projection and decoders are for image (text) generation. The two decoders jointly regularize the embeddings generated by the encoders and pull them into the same space. Further, we investigate information exchange for text-vision modalities and propose *CrossTransformer*, which uses two Transformer (Vaswani et al., 2017) encoders with shared parameters as the backbone model. Specifically, we insert *cls*¹ into the beginning of the generated embedding vectors of texts and images by the encoder-decoder module, which are then fed into the two Transformer encoders for both modalities. Intuitively, we first need to learn the global contextual information of the input vectors in the shallow layers of the Transformer encoders and then exchange the well-learned knowledge between

modalities. After the multimodal fusion completes, the exchange can stop. Therefore, in CrossTransformer, we introduce two hyper-parameters μ and η , which denote the start layer and the end layer for information exchanging, respectively. In each exchanging layer, we select the tokens in one modality with the smallest attention scores to *cls* and replace their embeddings with the average of all token embeddings in the other modality. In this way, text-vision fusion can be automatically performed. Finally, we summarize our contributions as follows.

- We generalize the exchanging-based methods from vision-vision fusion to text-vision fusion and propose a novel exchanging-based model MuSE.
- We employ the image captioning task and the text-to-image generation task to capture the correlations between texts and images, which jointly regularize multimodal embeddings and pull them into the same space. We further design CrossTransformer, which exchanges knowledge between texts and images.
- We conduct extensive experiments to compare MuSE with other state-of-the-arts on the MNER and MSA tasks. Experimental results show the effectiveness of our method.

2 Related Works

2.1 Deep Multimodal Fusion

Deep multimodal fusion has recently received significant attention in deep multimodal learning (Bayouh et al., 2021; Guo et al., 2019). Early methods can be mainly divided into two categories (Baltrušaitis et al., 2018), namely aggregation-based methods (Hazirbas et al., 2016; Zeng et al., 2019; Valada et al., 2020) and alignment-based methods (Colombo et al., 2021; Song et al., 2020). For the former, they learn separate representations in each modality and directly aggregate the

¹The special token in Transformer that can be used to derive the sentence-level embedding.

learned representations from different modalities, which lacks the inter-modal communication. In contrast, alignment-based methods use regularization to align embedding distributions in different modalities, such as mutual information maximization (Colombo et al., 2021) and maximum mean discrepancy (Gretton et al., 2012; Shankar, 2021). However, these methods omit the intra-modal characteristics with simple distribution aligning (Song et al., 2020). While some works (Han et al., 2021; Ju et al., 2021) combine aggregation and alignment, they need fine-grained hierarchical design that could introduce the additional cost of computation and engineering. Another taxonomy of multimodal fusion (De Vries et al., 2017) concentrates on the fusion stage and a detailed analysis is given in (Nagrani et al., 2021). Different from all these methods, an exchanging-based method CEN (Wang et al., 2020) is proposed for multi-vision modalities, which can effectively handle the trade-off between inter-modal processing and intra-modal fusion. While there exist some extensions (Wang et al., 2021b; Jiang et al., 2022) to CEN, all these methods are limited in channel-exchanging and vision-vision fusion.

Due to the space limitation, we move the related works of MNER and MSA to the Appendix A.

3 Methodology

In this section, we propose a deep multimodal fusion model MuSE. As shown in Figure 2, MuSE is mainly composed of four functional components and we tag them by ①-④. The component ① is used to project the input texts and images into low-dimensional spaces, which includes a text encoder and an image encoder. Considering that multimodal data might be mapped into different spaces, we further present two embedding regularizers (see components ② and ③) to pull embeddings of multimodal inputs into the same space. These two regularizers are taken as decoders, which implement the text-to-image generation task and the image captioning task, respectively. After the embeddings of multimodal inputs are generated, we feed them into component ④, which is a Transformer-encoder-based module called CrossTransformer. CrossTransformer performs multimodal information exchanging and finally generates fused embeddings from multimodality. Details of each component will be introduced in the following.

3.1 Low-dimensional Projection and Embedding Regularization

We use an architecture of two encoder-decoders to project the inputs of textual (T) and visual (I) modalities into the same embedding space before exchanging-based fusion.

Low-dimensional Projection. We first employ two separate encoders to encode the input texts and images into low-dimensional embeddings, respectively:

$$\mathbf{T}_e = \text{TextEncoder}(T), \quad (1)$$

$$\mathbf{I}_e = \text{ImageEncoder}(I), \quad (2)$$

where TextEncoder can be a typical text representation model (e.g., BERT (Kenton and Toutanova, 2019)) and ImageEncoder can be a typical CNN model (e.g., ResNet (He et al., 2016)). Specifically, we set $\mathbf{T}_e, \mathbf{I}_e \in \mathbb{R}^{n \times d}$, where n is the text length and d is the embedding dimensionality.

Embedding Regularization. Since the inputs are in two modalities, they are generally projected into different spaces by Equation 2. Therefore, for information exchange from multimodalities, we first need to pull these embeddings into the same space. Empirically, we observe that texts can be captions of images while images can be generated from texts, as shown in Figure 3. To capture the correlations between texts and images, we specially design an image captioning task and a text-to-image generation task. These two tasks are implemented by two decoders, which jointly regularize the embeddings from the encoders. For the image captioning task, the encoder takes the image embedding as input and generates the caption text, while we do the opposite for the text-to-image generation task. The overall procedure is summarized as follows. First, similar as in (Zhang et al., 2021b), to enhance the generalization ability of the model, we add random noise to the embeddings of texts and images:

$$\mathbf{T}_n = \text{MLP}(\mathbf{T}_e + \mathcal{N}_t(0, 1)), \quad (3)$$

$$\mathbf{I}_n = \text{MLP}(\mathbf{I}_e + \mathcal{N}_i(0, 1)), \quad (4)$$

where $\mathcal{N}_t(0, 1)$ and $\mathcal{N}_i(0, 1)$ are Gaussian random noise for textual and visual modalities, respectively. Then we use two decoders to generate images \hat{I} and texts \hat{T} , respectively:

$$\hat{I} = \text{ImageDecoder}(\mathbf{T}_n), \quad (5)$$

$$\hat{T} = \text{TextDecoder}(\mathbf{I}_n), \quad (6)$$

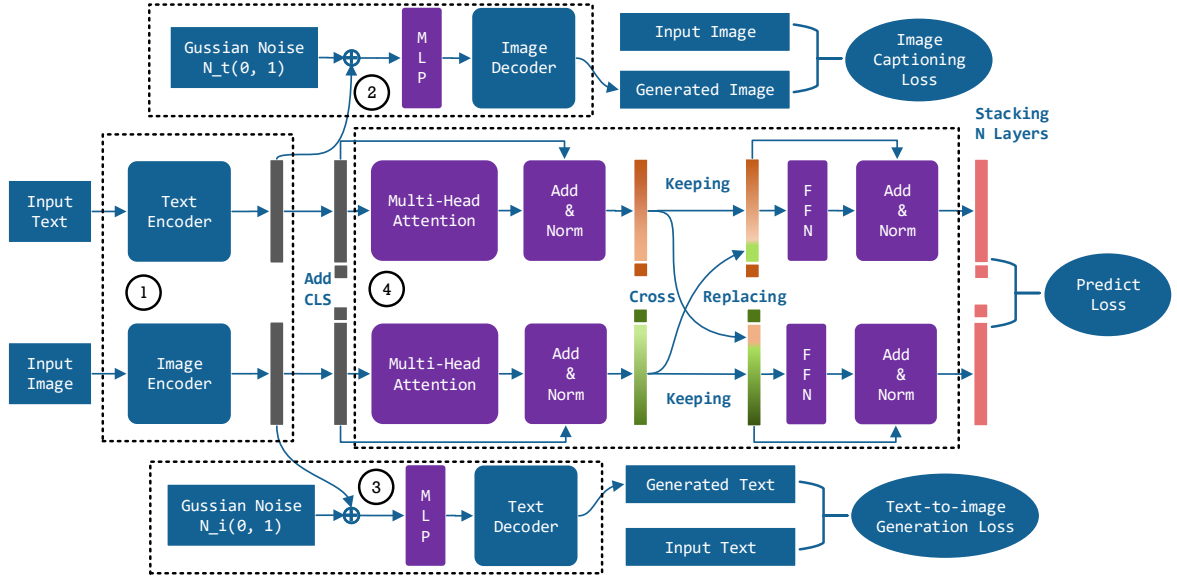


Figure 2: The overall architecture of MuSE.

where ImageDecoder can be a typical text-to-image generation model (e.g., PixelCNN (Van den Oord et al., 2016)), and TextDecoder can be a typical image captioning model (e.g., NIC (Vinyals et al., 2015)). Based on the generated images and texts, we compare them with the input ones and construct the text-to-image generation loss \mathcal{L}_{ti} and image captioning loss \mathcal{L}_{it} , respectively. These two losses regularize the embeddings of texts and images generated by the encoders and can be considered as auxiliary tasks to the main prediction task that will be introduced later.

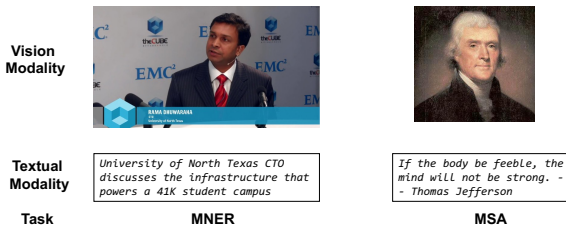


Figure 3: Toy examples on the correlations between texts and images, which are extracted from the Twitter15 (for the MNER task) and MVSA-Single (for the MSA task) datasets, respectively.

3.2 Multimodal Exchanging

After we derive embeddings \mathbf{T}_e and \mathbf{I}_e of textual and visual modalities, we next present the multimodal exchanging process. We start with the introduction of Transformer basics.

Transformer basics. Transformer (Vaswani et al., 2017) is introduced for sequential data modeling with an encoder-decoder structure. In Transformer, the inputs are linearly mapped to three matrices: query \mathbf{Q} , key \mathbf{K} , and value \mathbf{V} . The multi-head self-attention is then computed by:

$$\text{Attention}(\mathbf{Q}, \mathbf{K}, \mathbf{V}) = \text{Softmax}\left(\frac{\mathbf{Q}\mathbf{K}^T}{\sqrt{d_k}}\right)\mathbf{V}, \quad (7)$$

where $\sqrt{d_k}$ is the scaling factor. Here, $\text{Softmax}(\mathbf{Q}\mathbf{K}^T/\sqrt{d_k})$ generates an attention map matrix, which characterizes the attention scores between tokens. Generally, Transformer adds a special token cls to the beginning of the input sequences, which is used to derive the sentence-level embedding. Therefore, the first row of the attention map represents the attention scores of cls to all the tokens in the input. In this paper, we only use the Transformer encoder as in (Kenton and Toutanova, 2019), where each layer first computes the multi-head self-attention, followed by a feed-forward network (FFN) with residual connection (He et al., 2016) and layer normalization (Ba et al., 2016).

CrossTransformer. Based on Transformer, we propose CrossTransformer, which uses two Transformer encoders with shared parameters to learn the embeddings of textual and visual modalities, and exchanges information between multimodalities. The overall pipeline of CrossTransformer is shown in component ④ of Figure 2. We first add cls to the beginning of the embeddings generated by

the text encoder and the image encoder, which are taken as the input of the CrossTransformer. After that, considering that the global contextual information of both input vectors should be first learned and then exchanged, CrossTransformer sets its shallow layers as the regular Transformer encoder layer, followed by a number of exchanging layers. When multimodal fusion finishes, the exchanging process stops. To achieve this, CrossTransformer introduces two hyper-parameters μ and η to control the start layer and the end layer for information exchanging, respectively. In each exchanging layer, inspired by (Caron et al., 2021; Liang et al., 2022), we select tokens in one modality with a proportion of the smallest attention scores to *cls* and replace their embeddings vectors with the average embedding of all the tokens in the other modality. Here, *cls* is taken as the reference because it generates the sentence-level embedding.

Specifically, given the embeddings \mathbf{T}_e and \mathbf{I}_e generated from the text and image encoders, we first add *cls* to the beginning of them and obtain the inputs $\mathbf{T}_e(0), \mathbf{I}_e(0) \in \mathbb{R}^{(n+1) \times d}$ for CrossTransformer:

$$\mathbf{T}_e(0) = \text{Concat}(\mathbf{v}_{cls}(t_0), \mathbf{T}_e), \quad (8)$$

$$\mathbf{I}_e(0) = \text{Concat}(\mathbf{v}_{cls}(i_0), \mathbf{I}_e), \quad (9)$$

where $\mathbf{v}_{cls}(t_0)$ and $\mathbf{v}_{cls}(i_0)$ denote the initial embeddings of *cls* for textual and visual modalities, respectively. Here, n is the input text length and d is the embedding dimensionality. After μ regular Transformer encoder layers, we can obtain the updated embeddings $\mathbf{T}_e(\mu)$ and $\mathbf{I}_e(\mu)$. At layer $\mu+1$, we step into the exchanging layer, which consists of three sub-modules. The first sub-module calculates the multi-head self-attention in Equation 7, which generates intermediate embeddings $\tilde{\mathbf{T}}_e(\mu+1)$ for texts and $\tilde{\mathbf{I}}_e(\mu+1)$ for images. The second sub-module selects a θ -proportion of tokens with the smallest attention scores to *cls* for both modalities and performs information exchanging. Suppose the token corresponding to the k -th row of $\tilde{\mathbf{T}}_e(\mu+1)$ is selected, whose embedding vector is then updated by:

$$\begin{aligned} \tilde{\mathbf{T}}_e(\mu+1)[k, :] &= \frac{1}{n} \sum_{j=1}^n \tilde{\mathbf{I}}_e(\mu+1)[j, :] \\ &+ \tilde{\mathbf{T}}_e(\mu+1)[k, :], \end{aligned} \quad (10)$$

where we employ residual connection (He et al., 2016) to reduce the information loss caused by

replacement. Similarly, we can update the embedding vector in $\tilde{\mathbf{I}}_e(\mu+1)$ by:

$$\begin{aligned} \tilde{\mathbf{I}}_e(\mu+1)[k, :] &= \frac{1}{n} \sum_{j=1}^n \tilde{\mathbf{T}}_e(\mu+1)[j, :] \\ &+ \tilde{\mathbf{I}}_e(\mu+1)[k, :]. \end{aligned} \quad (11)$$

After information exchange, the third sub-module inputs the updated embedding matrices into FFN with layer normalization to obtain the output embeddings at layer $\mu+1$:

$$\mathbf{T}_e(\mu+1) = \text{FFN}(\tilde{\mathbf{T}}_e(\mu+1)), \quad (12)$$

$$\mathbf{I}_e(\mu+1) = \text{FFN}(\tilde{\mathbf{I}}_e(\mu+1)). \quad (13)$$

The exchanging process continues until reaching the preset end layer η . Finally we concatenate the output embeddings of the two Transformers and feed them into a fully connected network to derive the final fusion embedding matrix \mathbf{F}_e .

3.3 Training Objective

The overall optimization objective function of MuSE is summarized as

$$\mathcal{L} = \mathcal{L}_{task} + \alpha \mathcal{L}_{it} + \beta \mathcal{L}_{ti}, \quad (14)$$

where \mathcal{L}_{task} , \mathcal{L}_{it} , \mathcal{L}_{ti} are the loss of the main task (MNER or MSA), the image captioning task and the text-to-image generation task, respectively. Here, α and β are two hyper-parameters to balance the importance of the three terms.

4 Experiments

In this section, we evaluate the performance of MuSE by comparing it with other multimodal fusion methods on two tasks: Multimodal Named Entity Recognition (MNER) and Multimodal Sentiment Analysis (MSA). Given an input pair of text T and image I , MNER aims to extract a set of entities from T and classify each entity into one of the pre-defined types; the target of MSA is to classify each pair to one of the pre-defined sentiment types.

Common Implementation. Before diving into the details of experiments, we introduce the common implementation in two tasks. We use ResNet (He et al., 2016), BERT (Kenton and Toutanova, 2019), PixelCNN++ (Salimans et al., 2017), NIC-Att (Xu et al., 2015) for ImageEncoder, TextEncoder, ImageDecoder, TextDecoder, respectively. The batch size is set to 40, and the learning

rate is selected via a small grid search [1e-4, 5e-5, 1e-5] on the validation set. In ImageEncoder, the input image is resized to [224, 224] and the encoded image size is set to [8, 8]. In TextEncoder, the max sequence length is set to 64. In ImageDecoder, the input image is resized to [32, 32]. In CrossTransformer, we keep the same setting with Transformer encoder, except that the dropout rate is selected via a small grid search [0.1, 0.2, 0.3, 0.4] on the validation set. For loss selection, we use CrossEntropy for MNER prediction, MSA prediction and image captioning, and use discretized mix logistic loss for text-to-image generation as in PixelCNN++. For initialization of *cls*, we use Kaiming Initialization (He et al., 2015). Our framework is implemented based on PyTorch (Paszke et al., 2019). We run all experiments on 6 Tesla V100 GPUs.

Due to the space limitation, we move the description of datasets to Appendix B.

4.1 Multimodal Named Entity Recognition

Implementation. Following previous works (Yu et al., 2020), we feed the generated fusion embedding F_e into a CRF (Lafferty et al., 2001) layer to make prediction for MNER. The learning rate and the dropout rate of CRF are set to 0.0001 and 0.5, respectively.

Results. We compare our method with three types of competitors: aggregation-based methods (GVATT (Lu et al., 2018), AdaCAN (Zhang et al., 2018), UMT (Yu et al., 2020)), alignment-based methods (ITA (Wang et al., 2021a)), and task-specific methods (RIVA (Sun et al., 2020), RpBERT (Sun et al., 2021), UMGF (Zhang et al., 2021a)). Details of these approaches can be found in Section A.1. We take precision, recall and F1 score as the evaluation measures. For all the measures, the larger value indicates the better model performance. Table 1 summarizes the comparison results. From the table, we see that MuSE achieves the best performance w.r.t. all the evaluation metrics on all the datasets. In particular, MuSE leads the runner-up w.r.t. the F1 score by percents of 1.29 and 1.22 on Twitter15 and Twitter17, respectively. These results demonstrate the effectiveness of our exchanging-based method for multimodal fusion. Further, we notice that in MT-product, our method is the only one that can beat BERT-CRF, which also justifies the generalizability of MuSE.

Due to the space limitaion, we move the effi-

ciency analysis on MNER datasets to Appendix C.

4.2 Multimodal Sentiment Analysis

Implementation. We apply a one-layer MLP on the fusion embedding of the *cls* token to classify the sentiments in MSA. The dropout rate of the MLP is set to 0.5.

Results. We compare MuSE with two types of approaches: aggregation-based methods (CNN-Multi (Cai and Xia, 2015), DNN-LR (Yu et al., 2016), HSAN (Xu, 2017), MultiSN (Xu and Mao, 2017), MVAN (Yang et al., 2020)), and alignment-based methods (ITIN (Zhu et al., 2022), CoMN (Xu et al., 2018)), whose details are provided in Section A.2. We choose accuracy and F1 score as evaluation metrics. For both metrics, the larger the value, the better the model performance. The results are given in Table 2. From the table, we observe that MuSE outperforms other competitors on both datasets. In particular, compared with the runner-up model ITIN that is based on inter-modal alignment, MuSE utilizes both the intra-modal processing and inter-modal exchanging-based fusion, which explains its superiority.

4.3 Ablation Study

We further conduct an ablation study to verify the importance of the main components in MuSE. Specifically, one variant takes only the textual input. We call this variant **MuSE-only-T**. Similarly, we define another variant **MuSE-only-I** that inputs only the vision modality. These two variants help us recognize the importance of multimodal fusion for downstream tasks. To further show the significance of CrossTransformer, we remove it from MuSE and directly employ the embeddings generated from TextEncoder and ImageEncoder. We call this variant **MuSE-w/o-CT**. Finally, To show the necessity of the image captioning task and the text-to-image generation task for embedding regularization, we propose three variants, in which **MuSE-only- \mathcal{L}_{task}** only optimizes the task loss, **MuSE-w/o- \mathcal{L}_{it}** removes the image captioning loss, and **MuSE-w/o- \mathcal{L}_{ti}** removes the text-to-image generation loss.

Table 3 summarizes the results w.r.t. the F1 score on both MNER and MSA tasks. From the table, we see that: 1) MuSE clearly outperforms MuSE-only-T and MuSE-only-I, which shows the importance of multimodal fusion for textual and visual representation in the MNER and MSA tasks. 2) MuSE

Table 1: MNER results (%) w.r.t. precision (P), recall (R) and F1 scores. We highlight the best results in bold. * indicates that the improvements are statistically significant for $p < 0.01$ with paired t-test.

| Methods | Twitter15 | | | Twitter17 | | | MT-Product | | |
|-----------------------------|--------------|--------------|--------------|--------------|--------------|--------------|--------------|--------------|---------------|
| | P | R | F1 | P | R | F1 | P | R | F1 |
| BERT-CRF | 69.22 | 74.59 | 71.81 | 83.32 | 83.57 | 83.44 | 45.13 | 42.94 | 44.01 |
| GVATT (Lu et al., 2018) | 73.96 | 67.90 | 70.80 | 83.14 | 80.38 | 81.87 | - | - | - |
| AdaCAN (Zhang et al., 2018) | 72.75 | 68.75 | 70.69 | 84.16 | 80.24 | 82.15 | 40.15 | 41.66 | 40.89 |
| UMT (Yu et al., 2020) | 71.67 | 75.23 | 73.41 | 85.28 | 85.34 | 85.31 | 40.86 | 43.69 | 42.22 |
| RIVA (Sun et al., 2020) | - | - | 73.80 | - | - | 87.40 | - | - | - |
| RpBERT (Sun et al., 2021) | - | - | 74.40 | - | - | 87.40 | - | - | - |
| UMGF (Zhang et al., 2021a) | 74.49 | 75.21 | 74.85 | 86.54 | 84.50 | 85.51 | 41.67 | 43.55 | 42.58 |
| ITA (Wang et al., 2021a) | - | - | 75.52 | - | - | 85.96 | - | - | - |
| MuSE | 76.13 | 77.51 | 76.81 | 88.92 | 88.32 | 88.62 | 49.17 | 40.34 | 44.32* |

Table 2: MSA results (%) w.r.t. accuracy and F1 scores. We highlight the best results in bold. * indicates that the improvements are statistically significant for $p < 0.01$ with paired t-test.

| Methods | MVSA-Single | | MVSA-Multiple | |
|-------------------------------|---------------|---------------|---------------|---------------|
| | Accuracy | F1 | Accuracy | F1 |
| CNN-Multi (Cai and Xia, 2015) | 61.20 | 58.37 | 66.39 | 64.19 |
| DNN-LR (Yu et al., 2016) | 61.42 | 61.03 | 67.86 | 66.33 |
| HSAN (Xu, 2017) | - | 66.90 | - | 67.76 |
| MultiSN (Xu and Mao, 2017) | 69.84 | 69.63 | 68.86 | 68.11 |
| CoMN (Xu et al., 2018) | 70.51 | 70.01 | 69.92 | 69.83 |
| MVAN (Yang et al., 2020) | 72.98 | 72.98 | 72.36 | 72.30 |
| ITIN (Zhu et al., 2022) | 75.19 | 74.97 | 73.52 | 73.49 |
| MuSE | 75.80* | 75.58* | 74.10* | 73.93* |

achieves better performance than MuSE-w/o-CT. This is because CrossTransformer performs multimodal knowledge exchanging, which boosts the quality of the learned embeddings for each modality. 3) The outperformance of MuSE over the remaining three variants shows the necessity of embedding regularization. Since multimodal data could be projected into different spaces, both the image captioning task and the text-to-image generation task are used to pull embeddings of multimodalities into the same space, based on which multimodal fusion can then be performed. To conclude, all the components in MuSE are important.

4.4 Hyper-parameter Sensitivity Analysis

We end this section with a sensitivity analysis of hyper-parameters in our model. In particular, we investigate three key hyper-parameters in CrossTransformer: the exchange proportion θ of tokens, the start layer μ and the end layer η for multimodal

exchanging. We study one hyper-parameter with others fixed. Figure 4 shows the experimental results w.r.t. the F1 score on all the datasets. From the figure, our observations can be summarized as follows.

The exchange proportion θ . As shown in Figure 4a, the hyper-parameter θ plays an important role in MuSE. We see that the model performance first increases and then drops, with the increase of θ . When the θ is too small, the inter-modal fusion could be inadequate, which adversely affects the model performance. Further, when θ is too large, a large number of tokens will be replaced, which might attenuate the raw intra-modal knowledge. Our results empirically suggest that setting θ to be about 10% to 20% could be a reasonable choice. In our experiments, the default setting of θ is 10%.

The start layer μ . Since the default number of layers in the regular Transformer is 6, we vary the

Table 3: Ablation study results (%) on MuSE w.r.t. the F1 score. We highlight the best results in bold.

| Methods | Twitter15 | Twitter17 | MT-Product | MVSA-Single | MVSA-Multiple |
|---------------------------------|--------------|--------------|--------------|--------------|---------------|
| MuSE-only- T | 72.05 | 84.32 | 43.65 | 63.85 | 61.97 |
| MuSE-only- I | - | - | - | 64.99 | 62.39 |
| MuSE-w/o-CT | 73.26 | 85.46 | 43.78 | 74.24 | 72.35 |
| MuSE-only- \mathcal{L}_{task} | 74.39 | 87.63 | 44.20 | 74.66 | 72.95 |
| MuSE-w/o- \mathcal{L}_{it} | 75.43 | 88.41 | 44.02 | 75.23 | 73.46 |
| MuSE-w/o- \mathcal{L}_{ti} | 75.27 | 88.10 | 44.13 | 75.44 | 73.65 |
| MuSE | 76.81 | 88.62 | 44.32 | 75.58 | 73.93 |

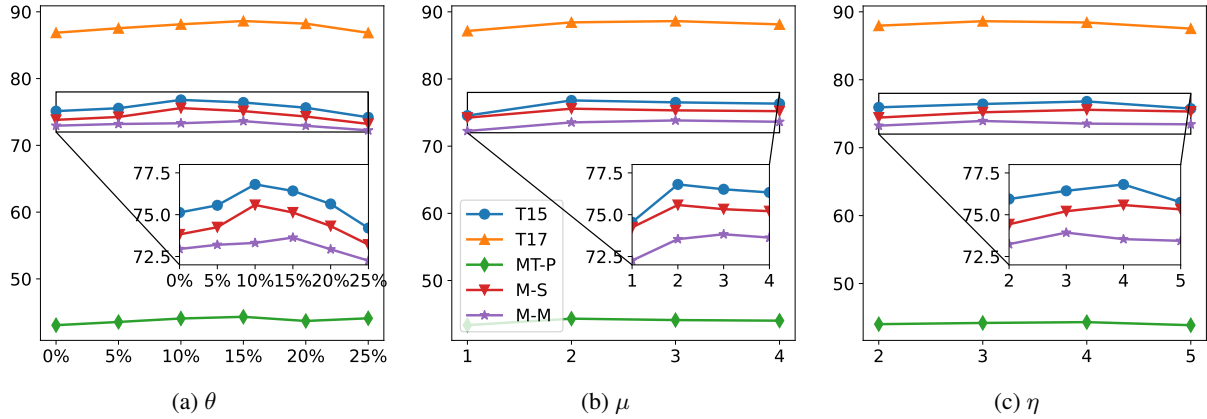


Figure 4: Hyper-parameter sensitivity analysis on the exchange proportion θ , the start layer μ and the end layer η for information exchanging in CrossTransformer. We short Twitter15, Twitter17, MT-Product, MVSA-Single, and MVSA-Multiple as T15, T17, MT-P, M-S, and M-M, respectively.

value of μ from $\{1, 2, 3, 4\}$. For any μ value, we fix the end layer η to 4. From Figure 4b, we observe that the model performance improves quickly when μ increases from 1 to 2. A possible explanation is that the randomly initialized embeddings for *cls* might not capture the sentence-level semantics and better contextual representations can be learned with few layers. This further demonstrates the necessity to use the regular Transformer layer without exchanging for contextual learning in the shallow layers of CrossTransformer.

The end layer η . We fix the start layer μ to 2 and show the results w.r.t. the end layer η in Figure 4c. Similar as in Figure 4b, we also see that the model performance first rises and then degenerates, as η increases. Within exchanging layers, MuSE fuses knowledge extracted from one modality to the other, which improves the quality of the learned representations and explains the performance increase. However, after the fusion completes, more exchanging layers could degrade the original intra-modal knowledge, which could lead to performance degeneration. We empirically set the default setting

of η to 4 in the experiments.

5 Conclusion

In this paper, we proposed a novel exchanging-based model MuSE for multimodal fusion. MuSE first uses two encoders to project inputs of texts and images into separate low-dimensional spaces. Then it regularizes the embeddings and pulls them into the same space with two generative decoders, which capture the correlations between texts and images by two tasks: image captioning and text-to-image generation. After that, based on the regularized embeddings, we proposed CrossTransformer for multimodal fusion by exchanging token embeddings from different modalities. We conducted extensive experiments to evaluate the performance of MuSE on MNER and MSA tasks. Experimental results show that our method performs favorably against other SOTAs.

6 Limitation

In this paper, we propose a new exchange-based multimodal fusion method that does better on the MNER and MSA tasks. Moreover, the hyperparameters of the exchange module are analyzed in detail. In the future, we will extend this method to more tasks.

7 Ethical Considerations

The proposed method has no obvious potential risks. All the scientific artifacts used/created are properly cited/licensed, and the usage is consistent with their intended use. Also, we open up our codes and hyper-parameters to facilitate future reproduction without repeated energy cost.

References

- Jimmy Lei Ba, Jamie Ryan Kiros, and Geoffrey E Hinton. 2016. Layer normalization. *arXiv preprint arXiv:1607.06450*.
- Tadas Baltrušaitis, Chaitanya Ahuja, and Louis-Philippe Morency. 2018. Multimodal machine learning: A survey and taxonomy. *IEEE transactions on pattern analysis and machine intelligence*, 41(2):423–443.
- Khaled Bayouddh, Raja Knani, Fayçal Hamdaoui, and Abdellatif Mtibaa. 2021. A survey on deep multimodal learning for computer vision: advances, trends, applications, and datasets. *The Visual Computer*, pages 1–32.
- Guoyong Cai and Binbin Xia. 2015. Convolutional neural networks for multimedia sentiment analysis. In *Natural language processing and chinese computing*, pages 159–167. Springer.
- Mathilde Caron, Hugo Touvron, Ishan Misra, Hervé Jégou, Julien Mairal, Piotr Bojanowski, and Armand Joulin. 2021. Emerging properties in self-supervised vision transformers. In *Proceedings of the IEEE/CVF International Conference on Computer Vision*, pages 9650–9660.
- Pierre Colombo, Emile Chapuis, Matthieu Labeau, and Chloé Clavel. 2021. Improving multimodal fusion via mutual dependency maximisation. In *Proceedings of the 2021 Conference on Empirical Methods in Natural Language Processing*, pages 231–245.
- Harm De Vries, Florian Strub, Jérémie Mary, Hugo Larochelle, Olivier Pietquin, and Aaron C Courville. 2017. Modulating early visual processing by language. *Advances in Neural Information Processing Systems*, 30.
- Arthur Gretton, Karsten M Borgwardt, Malte J Rasch, Bernhard Schölkopf, and Alexander Smola. 2012. A kernel two-sample test. *The Journal of Machine Learning Research*, 13(1):723–773.
- Wenzhong Guo, Jianwen Wang, and Shiping Wang. 2019. Deep multimodal representation learning: A survey. *IEEE Access*, 7:63373–63394.
- Wei Han, Hui Chen, and Soujanya Poria. 2021. Improving multimodal fusion with hierarchical mutual information maximization for multimodal sentiment analysis. In *Proceedings of the 2021 Conference on Empirical Methods in Natural Language Processing*, pages 9180–9192.
- Caner Hazirbas, Lingni Ma, Csaba Domokos, and Daniel Cremers. 2016. FuserNet: Incorporating depth into semantic segmentation via fusion-based CNN architecture. In *Asian conference on computer vision*, pages 213–228. Springer.
- Kaiming He, Xiangyu Zhang, Shaoqing Ren, and Jian Sun. 2015. Delving deep into rectifiers: Surpassing human-level performance on imagenet classification. In *Proceedings of the IEEE international conference on computer vision*, pages 1026–1034.
- Kaiming He, Xiangyu Zhang, Shaoqing Ren, and Jian Sun. 2016. Deep residual learning for image recognition. In *Proceedings of the IEEE conference on computer vision and pattern recognition*, pages 770–778.
- Sergey Ioffe and Christian Szegedy. 2015. Batch normalization: Accelerating deep network training by reducing internal covariate shift. In *International conference on machine learning*, pages 448–456. PMLR.
- Zijie Jiang, Hajime Taira, Naoyuki Miyashita, and Masatoshi Okutomi. 2022. Self-supervised ego-motion estimation based on multi-layer fusion of rgb and inferred depth. *arXiv preprint arXiv:2203.01557*.
- Xincheng Ju, Dong Zhang, Rong Xiao, Junhui Li, Shoushan Li, Min Zhang, and Guodong Zhou. 2021. Joint multi-modal aspect-sentiment analysis with auxiliary cross-modal relation detection. In *Proceedings of the 2021 Conference on Empirical Methods in Natural Language Processing*, pages 4395–4405.
- Jacob Devlin Ming-Wei Chang Kenton and Lee Kristina Toutanova. 2019. Bert: Pre-training of deep bidirectional transformers for language understanding. In *Proceedings of NAACL-HLT*, pages 4171–4186.
- John Lafferty, Andrew McCallum, and Fernando CN Pereira. 2001. Conditional random fields: Probabilistic models for segmenting and labeling sequence data.
- Youwei Liang, Chongjian Ge, Zhan Tong, Yibing Song, Jue Wang, and Pengtao Xie. 2022. Not all patches are what you need: Expediting vision transformers via token reorganizations. *arXiv preprint arXiv:2202.07800*.
- Di Lu, Leonardo Neves, Vitor Carvalho, Ning Zhang, and Heng Ji. 2018. Visual attention model for name tagging in multimodal social media. In *Proceedings*

- of the 56th Annual Meeting of the Association for Computational Linguistics (Volume 1: Long Papers), pages 1990–1999.
- Seungwhan Moon, Leonardo Neves, and Vitor Carvalho. 2018. Multimodal named entity recognition for short social media posts. In *Proceedings of the 2018 Conference of the North American Chapter of the Association for Computational Linguistics: Human Language Technologies, Volume 1 (Long Papers)*, pages 852–860.
- Arsha Nagrani, Shan Yang, Anurag Arnab, Aren Jansen, Cordelia Schmid, and Chen Sun. 2021. Attention bottlenecks for multimodal fusion. *Advances in Neural Information Processing Systems*, 34.
- Teng Niu, Shiai Zhu, Lei Pang, and Abdulmotaleb El Saddik. 2016. Sentiment analysis on multi-view social data. In *International Conference on Multimedia Modeling*, pages 15–27. Springer.
- Adam Paszke, Sam Gross, Francisco Massa, Adam Lerer, James Bradbury, Gregory Chanan, Trevor Killeen, Zeming Lin, Natalia Gimelshein, Luca Antiga, et al. 2019. Pytorch: An imperative style, high-performance deep learning library. *Advances in neural information processing systems*, 32.
- Tim Salimans, Andrej Karpathy, Xi Chen, and Diederik P Kingma. 2017. Pixelcnn++: Improving the pixelcnn with discretized logistic mixture likelihood and other modifications. *arXiv preprint arXiv:1701.05517*.
- Shiv Shankar. 2021. Neural dependency coding inspired multimodal fusion. *arXiv preprint arXiv:2110.00385*.
- Sijie Song, Jiaying Liu, Yanghao Li, and Zongming Guo. 2020. Modality compensation network: Cross-modal adaptation for action recognition. *IEEE Transactions on Image Processing*, 29:3957–3969.
- Lin Sun, Jiquan Wang, Yindu Su, Fangsheng Weng, Yuxuan Sun, Zengwei Zheng, and Yuanyi Chen. 2020. Riva: a pre-trained tweet multimodal model based on text-image relation for multimodal ner. In *Proceedings of the 28th International Conference on Computational Linguistics*, pages 1852–1862.
- Lin Sun, Jiquan Wang, Kai Zhang, Yindu Su, and Fangsheng Weng. 2021. Rpbert: A text-image relation propagation-based bert model for multimodal ner. In *Proceedings of the AAAI Conference on Artificial Intelligence*, volume 35, pages 13860–13868.
- Abhinav Valada, Rohit Mohan, and Wolfram Burgard. 2020. Self-supervised model adaptation for multimodal semantic segmentation. *International Journal of Computer Vision*, 128(5):1239–1285.
- Aaron Van den Oord, Nal Kalchbrenner, Lasse Espeholt, Oriol Vinyals, Alex Graves, et al. 2016. Conditional image generation with pixelcnn decoders. *Advances in neural information processing systems*, 29.
- Ashish Vaswani, Noam Shazeer, Niki Parmar, Jakob Uszkoreit, Llion Jones, Aidan N Gomez, Łukasz Kaiser, and Illia Polosukhin. 2017. Attention is all you need. *Advances in neural information processing systems*, 30.
- Oriol Vinyals, Alexander Toshev, Samy Bengio, and Dumitru Erhan. 2015. Show and tell: A neural image caption generator. In *Proceedings of the IEEE conference on computer vision and pattern recognition*, pages 3156–3164.
- Xinyu Wang, Min Gui, Yong Jiang, Zixia Jia, Nguyen Bach, Tao Wang, Zhongqiang Huang, Fei Huang, and Kewei Tu. 2021a. Ita: Image-text alignments for multi-modal named entity recognition. *arXiv preprint arXiv:2112.06482*.
- Yikai Wang, Wenbing Huang, Fuchun Sun, Fengxiang He, and Dacheng Tao. 2021b. Channel exchanging networks for multimodal and multitask dense image prediction. *arXiv preprint arXiv:2112.02252*.
- Yikai Wang, Wenbing Huang, Fuchun Sun, Tingyang Xu, Yu Rong, and Junzhou Huang. 2020. Deep multimodal fusion by channel exchanging. *Advances in Neural Information Processing Systems*, 33:4835–4845.
- Yang Wu, Zijie Lin, Yanyan Zhao, Bing Qin, and Li-Nan Zhu. 2021. A text-centered shared-private framework via cross-modal prediction for multimodal sentiment analysis. In *Findings of the Association for Computational Linguistics: ACL-IJCNLP 2021*, pages 4730–4738.
- Kelvin Xu, Jimmy Ba, Ryan Kiros, Kyunghyun Cho, Aaron Courville, Ruslan Salakhudinov, Rich Zemel, and Yoshua Bengio. 2015. Show, attend and tell: Neural image caption generation with visual attention. In *International conference on machine learning*, pages 2048–2057. PMLR.
- Nan Xu. 2017. Analyzing multimodal public sentiment based on hierarchical semantic attentional network. In *2017 IEEE International Conference on Intelligence and Security Informatics (ISI)*, pages 152–154. IEEE.
- Nan Xu and Wenji Mao. 2017. Multisentinet: A deep semantic network for multimodal sentiment analysis. In *Proceedings of the 2017 ACM on Conference on Information and Knowledge Management*, pages 2399–2402.
- Nan Xu, Wenji Mao, and Guandan Chen. 2018. A co-memory network for multimodal sentiment analysis. In *The 41st international ACM SIGIR conference on research & development in information retrieval*, pages 929–932.
- Xiaocui Yang, Shi Feng, Daling Wang, and Yifei Zhang. 2020. Image-text multimodal emotion classification via multi-view attentional network. *IEEE Transactions on Multimedia*, 23:4014–4026.

- Jianfei Yu, Jing Jiang, Li Yang, and Rui Xia. 2020. Improving multimodal named entity recognition via entity span detection with unified multimodal transformer. In *Proceedings of the 58th Annual Meeting of the Association for Computational Linguistics*, pages 3342–3352.
- Yuhai Yu, Hongfei Lin, Jiana Meng, and Zhehuan Zhao. 2016. Visual and textual sentiment analysis of a microblog using deep convolutional neural networks. *Algorithms*, 9(2):41.
- Jin Zeng, Yanfeng Tong, Yunmu Huang, Qiong Yan, Wenxiu Sun, Jing Chen, and Yongtian Wang. 2019. Deep surface normal estimation with hierarchical rgb-d fusion. In *Proceedings of the IEEE/CVF Conference on Computer Vision and Pattern Recognition*, pages 6153–6162.
- Dong Zhang, Suzhong Wei, Shoushan Li, Hanqian Wu, Qiaoming Zhu, and Guodong Zhou. 2021a. Multi-modal graph fusion for named entity recognition with targeted visual guidance. In *Proceedings of the AAAI Conference on Artificial Intelligence*, volume 35, pages 14347–14355.
- Han Zhang, Jing Yu Koh, Jason Baldridge, Honglak Lee, and Yinfei Yang. 2021b. Cross-modal contrastive learning for text-to-image generation. In *Proceedings of the IEEE/CVF Conference on Computer Vision and Pattern Recognition*, pages 833–842.
- Qi Zhang, Jinlan Fu, Xiaoyu Liu, and Xuanjing Huang. 2018. Adaptive co-attention network for named entity recognition in tweets. In *Thirty-Second AAAI Conference on Artificial Intelligence*.
- Tong Zhu, Leida Li, Jufeng Yang, Sicheng Zhao, Hantao Liu, and Jiansheng Qian. 2022. Multimodal sentiment analysis with image-text interaction network. *IEEE Transactions on Multimedia*.

A Related Works

A.1 Multimodal Named Entity Recognition (MNER)

Existing works for MNER can be mainly categorized into three types: aggregation-based, alignment-based and task-specific. For example, AttMNER (Moon et al., 2018), GVATT (Lu et al., 2018) and AdaCAN (Zhang et al., 2018) are pioneering works that employ the attention mechanism to aggregate text and image features. UMT (Yu et al., 2020) further uses Transformer to enhance the aggregation performance. The alignment-based method ITA (Wang et al., 2021a) introduces three types of alignments between texts and images to improve the classification results. There are also some task-specific works, such as RIVA (Sun et al., 2020) and RpBERT (Sun et al., 2021), which aim to solve the mismatch problem between texts and images. Further, UMGF (Zhang et al., 2021a) proposes a unified multimodal graph fusion based on fine-grained graph modeling.

A.2 Multimodal Sentiment Analysis (MSA)

MSA has recently attracted growing attention for its capability in learning cross-domain knowledge for sentiment analysis. Similar as in MNER, there are also aggregation-based methods for MSA. For example, CNN-Multi (Cai and Xia, 2015) first uses three CNNs to learn visual and textual features and then aggregates them for sentiment prediction. Further, DNN-LR (Yu et al., 2016) introduces pre-trained CNNs to improve the performance. There also exist approaches (Xu, 2017; Xu and Mao, 2017; Yang et al., 2020) that present hierarchical designs to enhance aggregation networks. Another type of methods for MSA is based on aligning techniques. For example, CoMN (Xu et al., 2018) introduces mutual information to align the influences of texts and images; ITIN (Zhu et al., 2022) utilizes cross-modal alignment to capture the region-word correspondence with the adaptive gating module, which has been shown to achieve superior results.

B Datasets

B.1 MNER

We evaluate our method on two public datasets Twitter15 (Zhang et al., 2018) and Twitter17 (Lu et al., 2018), and we keep the same Train/Validation/Test splits. The two datasets are comprised of multimodal user posts, which are

collected from Twitter during 2014-2015 and 2016-2017, respectively. Each dataset contains four types of entities, namely person, location, organization and miscellaneous. We use the released version² from UMT (Yu et al., 2020). Additionally, we collected a product dataset MT-Product from a well-known E-commercial platform, which has only one type of entity, namely product. In this dataset, we only keep one sample for each product to ensure that products in the training and test sets do not overlap, to further test the model generalizability. We randomly split the dataset into the Training/Validation/Test sets with the split ratio 6/2/2. We will release this dataset later. The statistics of the three datasets are shown in Table 4.

B.2 MSA

We evaluate our method on two public datasets MVSA-Single and MVSA-Multiple³, which are released in (Niu et al., 2016). The two datasets are both collected from Twitter. For fair comparison, we preprocess the datasets following works (Xu and Mao, 2017; Zhu et al., 2022): 1) Remove the pairs whose image label and text label are inconsistent. 2) Split the datasets into the Training/Validation/Test sets randomly with the split ratio 8/1/1. Each dataset has three sentiment types, namely *positive*, *neutral*, and *negative*. The statistics of the two datasets are shown in Table 4.

C Efficiency Analysis

To evaluate the efficiency of MuSE, we compare it to several representative cross-attention-based text-vision fusion methods from the number of parameters (#Params), performance (Perf), training time in one epoch (TT), and evaluation time (ET). Table 5 gives the detailed comparison results. The results show that MuSE significantly improves performance on both datasets but also comes with higher time costs. Further, we can observe that the time cost of MuSE mainly comes from the exchanging module. We have rewritten the transformer layer of PyTorch but have not optimized it well. In the future, we will further optimize the code implementation.

²Twitter15 and Twitter17 download url: <https://github.com/jefferyYu/UMT>.

³MVSA-Single and MVSA-Multiple download url: <https://mcrlab.net/research/mvsa-sentiment-analysis-on-multi-view-social-data/>.

Table 4: The statistics of datasets.

| Task | Dataset | Training | Validation | Test |
|-------------------------------------|---------------|----------|------------|------|
| Multimodal Named Entity Recognition | Twitter15 | 4000 | 1000 | 3257 |
| | Twitter17 | 3373 | 723 | 723 |
| | MT-Product | 2680 | 893 | 895 |
| Multimodal Sentiment Analysis | MVSA-Single | 3600 | 440 | 471 |
| | MVSA-Multiple | 13600 | 1720 | 1707 |

Table 5: Efficiency comparison.

| Models(#Params) | T15 | | | T17 | | |
|-----------------------------|-------|------|-----|-------|------|-----|
| | Perf | TT | ET | Perf | TT | ET |
| ViLBERT + bilstm-crf (210M) | 73.88 | 90s | 12s | 87.23 | 78s | 8s |
| UMT (208M) | 73.41 | 86s | 10s | 85.31 | 74s | 7s |
| MuSE w/o two tasks (204M) | 74.39 | 145s | 28s | 87.63 | 118s | 27s |
| MuSE (236M) | 76.13 | 180s | 32s | 88.62 | 161s | 30s |